https://doi.org/10.5194/acp-2020-1031
Preprint. Discussion started: 30 November 2020

Atmospheric Chemistry and Physics Discussions

Measurement report: Comparison of wintertime individual particles at ground level and above the mixed layer in urban Beijing

Wenhua Wang[1, 2, 3], Longyi Shao[1*], Claudio Mazzoleni[3], Yaowei Li[1], Simone Kotthaus[4], Sue Grimmond[4], Janarjan Bhandari[3], Jiaoping Xing[1, 5], Xiaolei Feng[1], Mengyuan Zhang[1], Zongbo Shi[6]

1. State Key Laboratory of Coal Resources and Safe Mining & College of Geosciences and Surveying Engineering, China University of Mining and Technology, Beijing, 100083, China
2. School of Resources and Materials, Northeastern University at Qinhuangdao, Qinhuangdao, 066004, China
3. Atmospheric Sciences Program & Physics Department, Michigan Technological University, Houghton, 49931, USA
4. Department of Meteorology, University of Reading, Reading, RG6 6BB, UK
5. School of Forestry, Jiangxi Agricultural University, Nanchang, 330045, China
6. School of Geography Earth and Environmental Sciences, the University of Birmingham, Birmingham, B15 2TT, UK

* Corresponding author: ShaoL@cumtb.edu.cn

Abstract:

Beijing has been suffering from frequent severe air pollution events, with concentrations affected significantly by the mixed layer height. Major efforts have been made to study the physico-chemical properties, composition, and sources of aerosol particles at ground level. However, little is known on morphology, elemental composition, and mixing state of aerosol particles above the mixed layer. In this work, we collected individual aerosol particles simultaneously at ground level (2 m above ground) and above the mixed layer in urban Beijing (within the Atmospheric Pollution and Human Health in a Chinese Megacity (APHH-Beijing) 2016 winter campaign). The particles were analyzed off-line using transmission electron microscopy coupled with energy dispersive X-ray spectroscopy. Our results showed that the relative number contribution of mineral particles to all measured particles was much higher during non-haze periods (42.5%) than haze periods (18.1%); on the contrary, internally mixed particles contributed more during haze periods (21.9%) than non-haze periods (7.2%) at ground level. In addition, more mineral particles were found at ground level than above the mixed layer height. Around 20% of individual particles showed core-shell structures during haze periods, whereas only a few core-shell particles were observed during non-haze periods (2%). We found that the particle above the mixed layer tend to be more aged with a larger proportion of organic particles originated from coal combustion. Our results indicate that a significant fraction of the airborne particles above the mixed layer originated from surrounding areas influenced by coal combustion activities. This source contributes to the surface particle concentrations in Beijing when polluted air is mixed down to the ground level.

Keywords: haze; individual particle; organic particle; core-shell structure; mixed layer.

https://doi.org/10.5194/acp-2020-1031
Preprint. Discussion started: 30 November 2020

Atmospheric Chemistry and Physics Discussions

1. Introduction

Atmospheric aerosols, emitted from anthropogenic or natural sources, consist of various chemical constituents (e.g., organic matter, black carbon, nitrate, sulfate, ammonium, metals, mineral dust) (Merikallio et al., 2011; Guo et al., 2014;Wang et al., 2016; Peng et al., 2016; Shao et al., 2017; Tao et al., 2017). Anthropogenic aerosols have received increased attention in the last decades due to their effects on climate and the environment. In fact, anthropogenic aerosols affect climate through cloud condensation nuclei activity (Kerminen et al., 2012), hygroscopic growth (Brock et al., 2016), and light scattering and absorption (Jacobson, 2001; Bond and Bergstrom, 2006; Merikallio et al., 2011; China et al., 2013; Peng et al., 2016; Bhandari et al., 2019b). They can also adversely impact human health; for example, by carrying toxic and carcinogenic compounds (Chen et al., 2013; Shao et al., 2016, 2017). High concentrations of aerosol particles in urban air can cause cardiovascular, respiratory, and even nervous system diseases (Xia et al., 2018; De Marco et al., 2019; Shou et al., 2019). It is suggested that outdoor air pollution causes 3.3 million people premature deaths globally each year (Lelieveld et al., 2015). Atmospheric aerosol particles also affect regional and global geochemical cycles when they are transported over long distances (Heald et al., 2006; Weijun Li et al., 2017; Rodriguez-Navarro et al., 2018).

Recently, China has suffered from severe air pollution conditions, like other countries undergoing rapid social and economic development (Huang et al., 2014). In China, this has been associated with frequent occurrence of haze episodes, high $PM_{2.5}$ mass levels, and expanded haze areas (Guo et al., 2014; Huang et al., 2014; Sun et al., 2014). For example, the maximum hourly average $PM_{2.5}$ mass concentrations reached more than 1000 μg m^{-3} in Beijing winter time (Li et al., 2017a; Zhang et al., 2017), 40 times above the safe level of 25 μg m^{-3} recommended by the World Health Organization (WHO).

As the megacity capital, Beijing has received much attention being one of the most polluted cities in China. Atmospheric researchers have focused on aerosol particles to understand haze formation in China (Sun et al., 2013; Huang et al., 2014; Zhou et al., 2018b). Measurements and model analyses highlight the key roles of secondary aerosol formation by trace gases (e.g., volatile organic compounds, and SO_2, NO_x) and stagnant meteorological conditions in the regional haze formation (Wang et al., 2013; Guo et al., 2014; Huang et al., 2014).

https://doi.org/10.5194/acp-2020-1031
Preprint. Discussion started: 30 November 2020

Atmospheric Chemistry and Physics Discussions

As characterization of aerosol particles has focused on surface level observations, the knowledge of aerosol properties at higher altitudes in urban areas remains poor (Zhou et al., 2018a). Vertical differences between precursors, oxidants and temperature gradients may influence gas-particle partitioning and heterogeneous reactions of N_2O_5 (Zhou et al., 2018a). Previous Beijing measurements at the Institute of Atmospheric Physics (IAP) meteorological tower showed complex vertical distributions of particulate matter and gaseous pollutants (Meng et al., 2008; Sun et al., 2015; Wang et al., 2018; Zhou et al., 2018b), but most of these studies focused on non-refractory submicron species. Research showed that the mixed layer height (MLH) could explain some of the vertical difference of aerosol particle chemical composition (Sun et al., 2015; Wang et al., 2018). For example, vertical distributions of aerosol particles tend to be more uniform during periods with higher MLH (Wang et al., 2018). As heavily increased air pollution can reduce boundary layer heights by diminishing incoming solar energy and therefore, by weakening vertical turbulence, aerosol near-surface concentrations become elevated (Petaja et al., 2016). Moreover, the upper layer particles can influence those below in the MLH by downward entrainment or mixing plumes, making the lower layer particles more complex (Wehner et al., 2010; Platis et al., 2015; Qi et al., 2019). Previous studies showed that the particles above the MLH sometimes considerably influence cloud formation (Carnerero et al., 2018) and showed strong aerosol-radiation effect (Bond and Bergstrom, 2006). The differences in aerosol types at ground level and at higher altitudes can lead to large differences in aerosol direct forcing estimates (Ramanathan et al., 2002; Li et al., 2010). The vertical difference of aerosol particles also increases the uncertainties in the assessment of the climate system (Li et al., 2017b). Therefore, a detailed knowledge of the vertical distribution and chemical composition of aerosols is important for understanding the impact on climate and the aerosol evolution process (Zhang et al., 2009; Wang et al., 2018).

Vertical comparisons of individual aerosol particles and their morphology, mixing states, and elemental compositions are very limited. Transmission Electron Microscopy (TEM) can provide detailed individual particle characterization and help to explain heterogeneous reactions and aging process (Li et al., 2016a). In this study, we compare particles simultaneously collected at ground level and above the MLH based on the meteorological tower at IAP in Beijing, as part of the UK-CHINA atmospheric pollution and Human Health (APHH) 2016 winter campaign.

https://doi.org/10.5194/acp-2020-1031
Preprint. Discussion started: 30 November 2020

Atmospheric Chemistry and Physics Discussions

2. Experimental

2.1. Aerosol sampling

Individual aerosol samples were collected at the tower division of IAP, Chinese Academy of Science (39°58′N, 116°22′E), in Beijing from 1 to 9 December of 2016. The site, located between the north 3rd and 4th ring roads in Beijing, is influenced by surrounding and regional traffic, and commercial, as well as, residential activities (Sun et al., 2016).

Two DKL-2 single stage cascade impactors, with a 0.5-mm-diameter jet nozzle and a flow rate of 1 L min^{-1} were used. The sampler collection efficiency is ~ 100% at an aerodynamic diameter of 0.5 μm if the particle density is 2 $g \cdot cm^{-3}$ (Li et al., 2016b). Copper (Cu) TEM grids, coated with carbon film (300-mesh; Tianld Co.; Beijing, China), were used to collect the aerosol samples. The sampling duration ranged from 30 second to less than 5 minutes depending on the air pollution loads. Simultaneous observation at ground level (Z1; 2 m above ground) and an elevated altitude (Z2; 280 m above ground) allowed us for the vertical profile of the characteristics of the particles to collected. The collected samples were stored in a dry plastic tube and placed in an air dryer to minimize particle changes before analysis.

Automatic Lidar and Ceilometer (ACL) observations of attenuated backscatter were conducted at the site using a Vaisala CL31 sensor. Measurements were corrected to account for instrument-related background and near range artefacts (Kotthaus et al., 2016). The MLH was derived from profile measurements using the automatic CABAM algorithm (Kotthaus and Grimmond, 2018). Since the TEM samples were collected for less than 5 minutes, the MLH at 15 min resolution was used to determine whether the Z2 observations were located within the MLH or above the MLH (Shi et al., 2019).

Samples were obtained during the periods shown (solid dots and dashed lines) in Fig. 1a; detailed sample information is provided in Table 1. Other measurements including $PM_{2.5}$, SO_2, NO_2, and O_3 mass concentrations at ground level were obtained from the Olympic Park monitor site, which is the closest national air quality monitor station to IAP (~1.5 km) (Shi et al., 2019). City average temperature (T) and relative humidity (RH) at ground level were obtained from the Ministry of Ecology and Environment of China (https://www.aqistudy.cn/).

2.2. Individual particle analysis

https://doi.org/10.5194/acp-2020-1031
Preprint. Discussion started: 30 November 2020

Atmospheric Chemistry and Physics Discussions

Individual particles were analyzed using a JEOL JEM-2800 TEM at an accelerating voltage of 200 kV. The morphology and mixing state of individual particles were determined from the TEM images. Semi-quantitative elemental composition was determined using Energy Dispersive X-ray Spectroscopy (EDS), by which elements heavier than Boron ($Z \geqslant 6$) can be detected. Cu is not included in this paper because the TEM grids were made of copper. The aerosol particles were not evenly distributed on the TEM grids; the coarser particles occurred near the center and the finer particles occurred on the periphery. To ensure a representative data analysis, three or four areas from the center to the periphery were selected and analyzed. The EDS collection duration of each individual particle was about 15 s to reduce damage of particles from the electron beam. The projected areas of individual particles were determined using the Image-J software (Schneider et al., 2012), which is commonly used for counting and measuring the projected area of atmospheric particles acquired by electron microscopes (Unga et al., 2018). First, the gray-scale images of the particles were converted into binary images, in which black pixels represent the particles and white pixels represent the background. The area equivalent diameters (D_{Aeq}) of the particles were calculated by the following formula: $D_{Aeq} = 2 \cdot (A/\pi)^{1/2}$, where A is the projected area of the particles shown in the TEM image.

3. Results and discussions

3.1. Air pollutants mass concentrations

The temporal variations of different air pollutants and meteorological conditions at ground level are shown in Fig. 1. The hourly averaged $PM_{2.5}$ mass concentration at the Olympic Park monitoring site ranged from 3 to 530 μg m^{-3}, with a sample period average of 113.3 μg m^{-3}, significantly exceeding the safe level of 75 μg m^{-3} according to the Chinese National Ambient Air Quality Standard (GB3095-2012). The MLH ranged from 54 to 1496 m, with an average of 397 m. The MLH showed obvious daily cycles. The hourly mean RH ranged from 17% to 97%, with a 9 day mean of 50.3%. The RH and $PM_{2.5}$ are positively correlated (correlation coefficient=0.75; Fig. S1) according to the 216 groups of hourly data, suggesting that the higher RH favors the formation of haze (Sun et al., 2014;Wang et al., 2016). As expected, RH and temperature were negatively correlated (correlation coefficient=-0.51; Fig. S2). The SO_2 time series has similar trends to that of NO_2. However, the average concentration of NO_2 (83.2 μg m^{-3}) was nearly 5.5 times higher than

https://doi.org/10.5194/acp-2020-1031
Preprint. Discussion started: 30 November 2020

Atmospheric Chemistry and Physics Discussions

that of SO_2 (15.2 μg m^{-3}). The concentration of O_3 showed a different trend compared with NO_2 and SO_2 (Fig. 1), with a 9 days hourly mean concentration of 20 μg m^{-3}.

3.2. Classification and mixing state of individual particles

Aerosol particles were classified using their morphologies and elemental compositions into seven main types, namely: 1) organic particles (OPs), 2) sulfur-rich (S-rich) particles, 3) soot particles, 4) mineral particles, 5) metal particles, 6) internally mixed organic and sulfur-rich particles (OP-S), and 7) other mixed particles. The detailed characteristics of each particle type are shown in Table 2.

OPs are mainly composed of C and O, usually with a small amount of Si, S, Cl, and K. OPs are relatively stable under the electron beam irradiation. Based on the morphologies, OPs can be further divided into spherical (Fig. 2a) and irregularly shaped (Fig. 2b). They were mainly from combustion process of biomass and fossil fuel.

S-rich particles (Figs. 2c and 2d) are mainly composed of O, S, and N, and sometimes also contain some amount of K. S-rich particles are beam-sensitive and volatilize under strong beam irradiation. S-rich particles generally represent secondary inorganic components (e.g., SO_4^{2+}, NO_3^- and NH_4^+) (Xu et al., 2019).

Soot particles are mainly composed of C, minor amount of O, and sometimes Si. Soot particles consist of a number of C-dominated spherical monomers less than 100 nm in diameter (Figs. 2e and 2f) and can be easily identified under high-resolution TEM (Buseck et al., 2014; Bhandari et al., 2017). Soot particles, stable under the electron beam, show chain-like or compact morphology in the atmosphere (Sorensen et al., 2001; Adachi et al., 2007; China et al., 2013, 2015; Bhandari et al., 2019a). Soot particles are mainly generated during incomplete combustion of biomass and fossil fuel.

Metal particles (Figs. 2g and 2h) and Mineral particles (Fig. 2i) are stable under the beam irradiation. Mineral particles are mostly irregularly shaped containing crustal elements (e.g., Si, Al, Ca, Fe, Na, K, Mg, Ti, and S) in addition to O. They can be generated from windblown soil dust or road dust. Metal particles are spherical or near spherical and are mainly composed of Fe, Zn, Mn, Ti, and Pb. Metal particles ae mainly originating from industries, coal-fired power plants, and oil refineries (Xu et al., 2019) or vehicle brakes (Hou et al., 2018).

https://doi.org/10.5194/acp-2020-1031
Preprint. Discussion started: 30 November 2020

Atmospheric Chemistry and Physics Discussions

Internally mixed particles (Figs. 2j-p) are particles with at least two of the above components. They usually show relative larger diameter. We further classify them as internally mixed organic and sulfur-rich particles (OP-S) (Figs. 2j-l), and other mixed particles (Figs. 2m-p).

3.3. Ground level haze and non-haze individual particle comparison

Haze periods are defined as when the hourly average $PM_{2.5}$ mass concentration is more than 75 μg m^{-3}; the rest are defined as non-haze periods. A total of 1538 individual particles among 8 samples at ground level were analyzed based on the TEM results. The relative number percentage (N(type i)/ N(total)*100) of particles in each sample was calculated, and the results are provided in Table 3 and shown in Fig.3. During non-haze periods, the particles were composed of mineral particles (42.5%), OPs (21.1%), S-rich particles (20.0%), soot particles (6.4%), other mixed particles (5.6%), metal particles (2.83%), and OP-S (1.6%) in descending order. During haze periods, the particles were composed of OPs (28.3%), S-rich particles (23.5%), mineral particles (18.1%), OP-S (13.1%), other mixed particles (8.8%), soot particles (6.6%), and metal particles (1.7%) in descending order.

The mineral particles are mainly from re-suspended road dust, soil dust, and construction dust during non-desert transport dust episodes (Sun et al., 2006; Gao et al., 2016; Wang et al., 2017). The relative number percentage of mineral particles was much higher during non-haze periods (42.5%) than during haze periods (18.1%), as shown in Fig.3. However, the mixed particles including OP-S and other mixed particles were much more abundant during haze periods (21.9%) than during non-haze periods (7.2%), suggesting that there was more secondary aerosol formation during haze periods. High secondary aerosol formation in winter in Beijing during the pollution periods was also found in previous studies (Huang et al., 2014; Sun et al., 2016; Li et al., 2017a). Secondary aerosol formation is expected since the RH during the haze periods were relatively higher than during non-haze periods, as shown in Table 1 and Fig.1, which facilitated chemical reactions of gaseous pollutants (Liu et al., 2016; Wang et al., 2016). Also, the average OPs and S-rich were higher during haze periods than during non-haze periods.

3.4. Ground level and above the MLH individual particle comparison

A total of 1519 individual particles from 8 samples above the MLH were analyzed. The results are provided in Table 3 and shown in Fig. 3. During non-haze periods, the contribution of mineral

https://doi.org/10.5194/acp-2020-1031
Preprint. Discussion started: 30 November 2020

Atmospheric Chemistry and Physics Discussions

particles above the MLH (23.2%) was less than that at ground level (42.5%), but the S-rich and OPs accounted for 30.7% and 27.3% above the MLH, respectively, fractions higher than those of 20.0% and 21.1% at the ground level. During haze periods, the contribution of mineral particles above the MLH (9.5%) was also lower than at ground level (18.1%). S-rich particles were also less abundant above the MLH (16.4%) compared to the ground level (23.5%), which is different from the non-haze periods. This may be because more S-rich particles above the MLH were mixed with other particles, forming mixed particles. The mixed particles above the MLH were much higher than at ground level, especially the OP-S particles (20.7% vs 13.1%). OPs above the MLH (34.8%) were more abundant than at ground level (28.5%). Particles above the MLH were either transported from the surrounding areas or from ground sources. In both cases, they were subject to atmospheric process, leading to their aging.

3.5. Aging of particles

During the aging process of aerosol particles, secondary species can coat pre-existing particles (Li and Shao, 2009; Laskin et al., 2016; Li et al., 2016b; Niu et al., 2016; Tang et al., 2016; Chen et al., 2017; Hou et al., 2018; Unga et al., 2018; Xu et al., 2019). Using high-resolution TEM images, it is possible to identify the core-shell structure of particles (Li et al., 2016a). For example, Figs. 4a and 4b show S-rich particles coated by secondary species. Figs. 4c and 4d show Ops that were coated with secondary species. Figs. 4e-h show core-shell structured particles with some mixed particle cores. In this study, we found that the core-shell structured particles accounted for 20% during haze periods but only 2% during non-haze periods. Also, the average D_{Aeq} of particles was larger during haze periods than during non-haze periods as shown in Fig. S3. These results confirmed that particles during haze periods underwent more extensive aging than during non-haze periods.

The coating of atmospheric particles is often caused by aging mechanisms such as coagulation, condensation, and heterogeneous chemical reactions (Kahnert, 2015; Müller et al., 2017). Fig. 5 shows low magnification images of particles at ground level and above the MLH. The core/shell ratio (R), which is the ratio of the D_{Aeq} of the core to the D_{Aeq} of the whole particle including the coating, has been used to evaluate the aging process of aerosol particles in different studies (Niu et al., 2012, 2016; Hou et al., 2018). The value of R ranged from 0 to less than 1. A smaller R value

https://doi.org/10.5194/acp-2020-1031
Preprint. Discussion started: 30 November 2020


Atmospheric Chemistry and Physics Discussions

means the particles were more coated, thus were subjected to a more extensive degree of aging (Hou et al., 2018). Because a high number percentage of core-shell structured particles were only found during haze periods, we measured R of core-shell structured particles only during the haze periods (including the samples 2, 4, 5, 6 and 7). Fig. 6a shows the R value of each samples during the haze periods. The average R value above the MLH (0.54) was smaller than ground level (0.59). We can see from Fig. 6a that all the samples showed a smaller average R value above the MLH compared with those from the ground level. Additionally, the relative number percentage of core-shell structured particles was higher above the MLH than at ground level, except for sample 4. These findings indicate that the particles above the MLH were more aged than those at ground level.

4. Summary and Atmospheric implications

Our results show that mineral particles represented a higher number percentage during non-haze periods (42.5%) than during haze periods (18.1%), and mixed particles were more abundant in haze periods (21.9%) than in non-haze periods (7.2%) at the ground level. In addition, more mineral particles were found at ground level than above the MLH. Our results also show higher relative number percentage of OPs both during non-haze (21.1%) and haze periods (28.3%) in winter Beijing, compared with a tunnel environment (~5%), where the vehicle emissions were the main pollution sources (Hou et al., 2018). Also, recent studies did not find abundant OPs in North China during Spring and Summer (Yuan et al., 2015; Li et al., 2016b; Xu et al., 2019;). Instead, a larger number percentage of OPs have been found in winter using electron microscopy in previous studies, including an outflow of a haze plume in East Asia (Zhu et al., 2013), a coal-burning region in China's Loess Plateau (Li et al., 2012), three sampling sites in North China Plain (Chen et al., 2017) and urban and rural sites in Northeast China (Xu et al., 2017; Zhang et al., 2017). The results above suggest that OPs account for a large number percentage of the particles in north China in winter.

Most of the OPs in our study were spherical or nearly spherical in shape according to the projected images, suggesting that they were formed through cooling process after the biomass or fossil fuel combustion pyrolysis products of volatile organic compounds were emitted into the atmosphere (Wang et al., 2015; Chen et al., 2017; Zhang et al., 2017). These spherical or near spherical OPs were considered to be brown carbon (Zhang et al., 2020). Brown carbon plays a significant role in atmospheric shortwave absorption and can cause warming of the atmosphere

https://doi.org/10.5194/acp-2020-1031
Preprint. Discussion started: 30 November 2020

Atmospheric Chemistry and Physics Discussions

(Adachi and Buseck, 2011;Hoffer et al., 2016). Some researchers have found that the primary OPs from coal combustion has more Si than those from biomass burning (Li et al., 2012; Chen et al., 2017). The weight ratio of C-O-Si at ground level and above the MLH is shown in Fig. 7. More coal burning related OPs were found above the MLH. Since the relative number percentage of primary OPs affected by coal burning are higher above the MLH than at the ground level, the OPs above the MLH are not all from the ground level and might have originated from surrounding areas influenced by coal combustion. The particles above the MLH can contribute to Beijing air pollution by mixing down to the ground.

In this study, more core-shell structured particles were found above the MLH than at the ground; finding which can have important atmospheric implications. Fig. S3 shows the total particle number-size distribution; the larger size particles clearly increased when considering the coatings compared to only considering the core size during haze periods. The changes in optical properties due to coating was calculated in various studies by using different methods (Cappa et al., 2012; Scarnato et al., 2013; Liu et al., 2015; Saliba et al., 2016; Unga et al., 2018). When host particles are coated, their optical properties might be amplified. For example, when soot particles (optically often referred to as black carbon) are coated by secondary species, the light absorption is typically enhanced because of the so called “lensing effect” (Khalizov et al., 2009; Liu et al., 2009; Peng et al., 2016). Previous measurements showed that soot can heat the upper boundary layer more than the lower layer during haze periods and decrease surface heat flux substantially, thus depressing the development of MLH (Ding et al., 2016). Also, organic coating can influence the hygroscopic properties and the viscosity of mixed particles (Sharma et al., 2018; Unga et al., 2018), and thus can influence cloud formation activity (Kerminen et al., 2012).

The different relative number percentage of particle types and different aging degree of the particles have important implications for understanding the climate effects of aerosol particles and for emission control policy making.

Data availability: Data used in this study are available from the corresponding author upon request (ShaoL@cumtb.edu.cn)

Author Contributions: WW, LS, CM, JX and ZS conceived the manuscript. WW, WL, XF and MZ conducted the sample collection and analysis. SK and SG conducted the MLH measurement. CM and BJ conducted manuscript modification.

https://doi.org/10.5194/acp-2020-1031
Preprint. Discussion started: 30 November 2020

Atmospheric Chemistry and Physics Discussions

296 **Competing interest:** The authors declare no conflict of interest.

297 **Acknowledgements:** We thank Zifa Wang and Pingqing Fu at IAP for the supporting of sample
298 collection. This work was supported by National Natural Science Foundation of China (No.
299 42075107), International Cooperation Projects of National Natural Science Foundation of China
300 (No. 41571130031), Yue Qi Scholar Fund of China University of Mining and Technology (Beijing),
301 China Scholarship Council (No. 201806430015). CM and JB were supported by the U.S Department
302 of Energy (DOE), Office of Biological and Environmental Research (OBER), Atmospheric System
303 Research (#DE-SC0011935 and Grant # DE-SC0018931). ZS was supported by Natural
304 Environmental Research Council (NE/N007190/1).

https://doi.org/10.5194/acp-2020-1031
Preprint. Discussion started: 30 November 2020

Atmospheric Chemistry and Physics Discussions

Reference:

Adachi, K., Chung, S. H., Friedrich, H., and Buseck, P. R.: Fractal parameters of individual soot particles determined using electron tomography: Implications for optical properties, Journal of Geophysical Research, 112, 10.1029/2006jd008296, 2007.

Adachi, K., and Buseck, P. R.: Atmospheric tar balls from biomass burning in Mexico, J. Geophys. Res.-Atmos., 116, 7, 10.1029/2010jd015102, 2011.

Bhandari, J., China, S., Onasch, T., Wolff, L., Lambe, A., Davidovits, P., Cross, E., Ahern, A., Olfert, J., Dubey, M., and Mazzoleni, C.: Effect of Thermodenuding on the Structure of Nascent Flame Soot Aggregates, Atmosphere, 8, 10.3390/atmos8090166, 2017.

Bhandari, J., China, S., Chandrakar, K. K., Kinney, G., Cantrell, W., Shaw, R. A., Mazzoleni, L. R., Girotto, G., Sharma, N., Gorkowski, K., Gilardoni, S., Decesari, S., Facchini, M. C., Zanca, N., Pavese, G., Esposito, F., Dubey, M. K., Aiken, A. C., Chakrabarty, R. K., Moosmuller, H., Onasch, T. B., Zaveri, R. A., Scarnato, B. V., Fialho, P., and Mazzoleni, C.: Extensive Soot Compaction by Cloud Processing from Laboratory and Field Observations, Sci Rep, 9, 11824, 10.1038/s41598-019-48143-y, 2019a.

Bhandari, J., China, S., Girotto, G., Scarnato, B. V., Gorkowski, K., Aiken, A. C., Dubey, M. K., and Mazzoleni, C.: Optical properties and radiative forcing of fractal-like tar ball aggregates from biomass burning, Journal of Quantitative Spectroscopy and Radiative Transfer, 230, 65-74, 10.1016/j.jqsrt.2019.01.032, 2019b.

Bond, T. C., and Bergstrom, R. W.: Light Absorption by Carbonaceous Particles: An Investigative Review, Aerosol Science and Technology, 40, 27-67, 10.1080/02786820500421521, 2006.

Brock, C. A., Wagner, N. L., Anderson, B. E., Attwood, A. R., Beyersdorf, A., Campuzano-Jost, P., Carlton, A. G., Day, D. A., Diskin, G. S., Gordon, T. D., Jimenez, J. L., Lack, D. A., Liao, J., Markovic, M. Z., Middlebrook, A. M., Ng, N. L., Perring, A. E., Richardson, M. S., Schwarz, J. P., Washenfelder, R. A., Welti, A., Xu, L., Ziemba, L. D., and Murphy, D. M.: Aerosol optical properties in the southeastern United States in summer – Part 1: Hygroscopic growth, Atmospheric Chemistry and Physics, 16, 4987-5007, 10.5194/acp-16-4987-2016, 2016.

Buseck, P. R., Adachi, K., Gelencsér, A., Tompa, É., and Pósfai, M.: Ns-Soot: A Material-Based Term for Strongly Light-Absorbing Carbonaceous Particles, Aerosol Science and Technology, 48, 777-788, 10.1080/02786826.2014.919374, 2014.

Cappa, C. D., Onasch, T. B., Massoli, P., Worsnop, D. R., Bates, T. S., Cross, E. S., Davidovits, P., Hakala, J., Hayden, K. L., Jobson, B. T., Kolesar, K. R., Lack, D. A., Lerner, B. M., Li, S.-M., Mellon, D., Nuaaman, I., Olfert, J. S., Petäjä, T., Quinn, P. K., Song, C., Subramanian, R., Williams, E. J., and Zaveri, R. A.: Radiative Absorption Enhancements Due to the Mixing State of Atmospheric Black Carbon, Science, 337, 1078, 10.1126/science.1223447, 2012.

Carnerero, C., Pérez, N., Reche, C., Ealo, M., Titos, G., Lee, H.-K., Eun, H.-R., Park, Y.-H., Dada, L., Paasonen, P., Kerminen, V.-M., Mantilla, E., Escudero, M., Gómez-Moreno, F. J., Alonso-Blanco, E., Coz, E., Saiz-Lopez, A., Temime-Roussel, B., Marchand, N., Beddows, D. C. S., Harrison, R. M., Petäjä, T., Kulmala, M., Ahn, K.-H., Alastuey, A., and Querol, X.: Vertical and horizontal distribution of regional new particle formation events in Madrid, Atmospheric Chemistry and Physics, 18, 16601-16618, 10.5194/acp-18-

https://doi.org/10.5194/acp-2020-1031
Preprint. Discussion started: 30 November 2020

344 16601-2018, 2018.

345 Chen, S., Xu, L., Zhang, Y., Chen, B., Wang, X., Zhang, X., Zheng, M., Chen, J., Wang, W., Sun, Y., Fu, P.,
346 Wang, Z., and Li, W.: Direct observations of organic aerosols in common wintertime hazes in North China:
347 insights into direct emissions from Chinese residential stoves, Atmospheric Chemistry and Physics, 17,
348 1259-1270, 10.5194/acp-17-1259-2017, 2017.

349 Chen, Y., Ebenstein, A., Greenstone, M., and Li, H.: Evidence on the impact of sustained exposure to air
350 pollution on life expectancy from China's Huai River policy, Proc Natl Acad Sci U S A, 110, 12936-12941,
351 10.1073/pnas.1300018110, 2013.

352 China, S., Mazzoleni, C., Gorkowski, K., Aiken, A. C., and Dubey, M. K.: Morphology and mixing state of
353 individual freshly emitted wildfire carbonaceous particles, Nat Commun, 4, 2122,
354 10.1038/ncomms3122, 2013.

355 China, S., Mazzoleni, C., Gorkowski, K., Aiken, A.C. and Dubey, M.K., 2013. Morphology and mixing state
356 of individual freshly emitted wildfire carbonaceous particles. Nat Commun, 4: 2122.

357 China, S., Scarnato, B., Owen, R. C., Zhang, B., Ampadu, M. T., Kumar, S., Dzepina, K., Dziobak, M. P.,
358 Fialho, P., Perlinger, J. A., Hueber, J., Helmig, D., Mazzoleni, L. R., and Mazzoleni, C.: Morphology and
359 mixing state of aged soot particles at a remote marine free troposphere site: Implications for optical
360 properties, Geophysical Research Letters, 42, 1243-1250, 10.1002/2014gl062404, 2015.

361 De Marco, A., Proietti, C., Anav, A., Ciancarella, L., D'Elia, I., Fares, S., Fornasier, M. F., Fusaro, L., Gualtieri,
362 M., Manes, F., Marchetto, A., Mircea, M., Paoletti, E., Piersanti, A., Rogora, M., Salvati, L., Salvatori, E.,
363 Screpanti, A., Vialetto, G., Vitale, M., and Leonardi, C.: Impacts of air pollution on human and ecosystem
364 health, and implications for the National Emission Ceilings Directive: Insights from Italy, Environ Int, 125,
365 320-333, 10.1016/j.envint.2019.01.064, 2019.

366 Ding, A. J., Huang, X., Nie, W., Sun, J. N., Kerminen, V. M., Petäjä, T., Su, H., Cheng, Y. F., Yang, X. Q., Wang,
367 M. H., Chi, X. G., Wang, J. P., Virkkula, A., Guo, W. D., Yuan, J., Wang, S. Y., Zhang, R. J., Wu, Y. F., Song, Y.,
368 Zhu, T., Zilitinkevich, S., Kulmala, M., and Fu, C. B.: Enhanced haze pollution by black carbon in megacities
369 in China, Geophysical Research Letters, 43, 2873-2879, 10.1002/2016gl067745, 2016.

370 Gao, J., Peng, X., Chen, G., Xu, J., Shi, G. L., Zhang, Y. C., and Feng, Y. C.: Insights into the chemical
371 characterization and sources of PM(2.5) in Beijing at a 1-h time resolution, Sci Total Environ, 542, 162-
372 171, 10.1016/j.scitotenv.2015.10.082, 2016.

373 Guo, S., Hu, M., Zamora, M. L., Peng, J., Shang, D., Zheng, J., Du, Z., Wu, Z., Shao, M., Zeng, L., Molina,
374 M. J., and Zhang, R.: Elucidating severe urban haze formation in China, Proc Natl Acad Sci U S A, 111,
375 17373-17378, 10.1073/pnas.1419604111, 2014.

376 Heald, C. L., Jacob, D. J., Park, R. J., Alexander, B., Fairlie, T. D., Yantosca, R. M., and Chu, D. A.: Transpacific
377 transport of Asian anthropogenic aerosols and its impact on surface air quality in the United States,
378 Journal of Geophysical Research, 111, 10.1029/2005jd006847, 2006.

379 Hoffer, A., Toth, A., Nyiro-Kosa, I., Posfai, M., and Gelencser, A.: Light absorption properties of
380 laboratory-generated tar ball particles, Atmospheric Chemistry and Physics, 16, 239-246, 10.5194/acp-
381 16-239-2016, 2016.

https://doi.org/10.5194/acp-2020-1031
Preprint. Discussion started: 30 November 2020

Hou, C., Shao, L., Hu, W., Zhang, D., Zhao, C., Xing, J., Huang, X., and Hu, M.: Characteristics and aging of traffic-derived particles in a highway tunnel at a coastal city in southern China, Sci Total Environ, 619-620, 1385-1393, 10.1016/j.scitotenv.2017.11.165, 2018.

Huang, R. J., Zhang, Y., Bozzetti, C., Ho, K. F., Cao, J. J., Han, Y., Daellenbach, K. R., Slowik, J. G., Platt, S. M., Canonaco, F., Zotter, P., Wolf, R., Pieber, S. M., Bruns, E. A., Crippa, M., Ciarelli, G., Piazzalunga, A., Schwikowski, M., Abbaszade, G., Schnelle-Kreis, J., Zimmermann, R., An, Z., Szidat, S., Baltensperger, U., El Haddad, I., and Prevot, A. S.: High secondary aerosol contribution to particulate pollution during haze events in China, Nature, 514, 218-222, 10.1038/nature13774, 2014.

Jacobson, M. Z.: Strong radiative heating due to the mixing state of black carbon in atmospheric aerosols, Nature, 409, 695-697, 10.1038/35055518, 2001.

Kahnert, M.: Modelling radiometric properties of inhomogeneous mineral dust particles: Applicability and limitations of effective medium theories, Journal of Quantitative Spectroscopy and Radiative Transfer, 152, 16-27, 10.1016/j.jqsrt.2014.10.025, 2015.

Kerminen, V. M., Paramonov, M., Anttila, T., Riipinen, I., Fountoukis, C., Korhonen, H., Asmi, E., Laakso, L., Lihavainen, H., Swietlicki, E., Svenningsson, B., Asmi, A., Pandis, S. N., Kulmala, M., and Petäjä, T.: Cloud condensation nuclei production associated with atmospheric nucleation: a synthesis based on existing literature and new results, Atmospheric Chemistry and Physics, 12, 12037-12059, 10.5194/acp-12-12037-2012, 2012.

Khalizov, A. F., Xue, H., Wang, L., Zheng, J., and Zhang, R.: Enhanced Light Absorption and Scattering by Carbon Soot Aerosol Internally Mixed with Sulfuric Acid, The Journal of Physical Chemistry A, 113, 1066-1074, 10.1021/jp807531n, 2009.

Kotthaus, S., O'Connor, E., Münkel, C., Charlton-Perez, C., Haeffelin, M., Gabey, A. M., and Grimmond, C. S. B.: Recommendations for processing atmospheric attenuated backscatter profiles from Vaisala CL31 ceilometers, Atmos. Meas. Tech., 9, 3769-3791, 10.5194/amt-9-3769-2016, 2016.

Kotthaus, S., and Grimmond, C. S. B.: Atmospheric boundary-layer characteristics from ceilometer measurements. Part 1: A new method to track mixed layer height and classify clouds, Quarterly Journal of the Royal Meteorological Society, 144, 1525-1538, 10.1002/qj.3299, 2018.

Laskin, A., Gilles, M. K., Knopf, D. A., Wang, B., and China, S.: Progress in the Analysis of Complex Atmospheric Particles, Annu Rev Anal Chem (Palo Alto Calif), 9, 117-143, 10.1146/annurev-anchem-071015-041521, 2016.

Lelieveld, J., Evans, J. S., Fnais, M., Giannadaki, D., and Pozzer, A.: The contribution of outdoor air pollution sources to premature mortality on a global scale, Nature, 525, 367-371, 10.1038/nature15371, 2015.

Li, J., Du, H., Wang, Z., Sun, Y., Yang, W., Li, J., Tang, X., and Fu, P.: Rapid formation of a severe regional winter haze episode over a mega-city cluster on the North China Plain, Environ Pollut, 223, 605-615, 10.1016/j.envpol.2017.01.063, 2017a.

Li, W., and Shao, L.: Transmission electron microscopy study of aerosol particles from the brown hazes in northern China, Journal of Geophysical Research, 114, 10.1029/2008jd011285, 2009.

https://doi.org/10.5194/acp-2020-1031
Preprint. Discussion started: 30 November 2020

Atmospheric Chemistry and Physics Discussions

Li, W., Shi, Z., Zhang, D., Zhang, X., Li, P., Feng, Q., Yuan, Q., and Wang, W.: Haze particles over a coal-burning region in the China Loess Plateau in winter: Three flight missions in December 2010, Journal of Geophysical Research: Atmospheres, 117, n/a-n/a, 10.1029/2012jd017720, 2012.

Li, W., Shao, L., Zhang, D., Ro, C.-U., Hu, M., Bi, X., Geng, H., Matsuki, A., Niu, H., and Chen, J.: A review of single aerosol particle studies in the atmosphere of East Asia: morphology, mixing state, source, and heterogeneous reactions, Journal of Cleaner Production, 112, 1330-1349, 10.1016/j.jclepro.2015.04.050, 2016a.

Li, W., Sun, J., Xu, L., Shi, Z., Riemer, N., Sun, Y., Fu, P., Zhang, J., Lin, Y., Wang, X., Shao, L., Chen, J., Zhang, X., Wang, Z., and Wang, W.: A conceptual framework for mixing structures in individual aerosol particles, Journal of Geophysical Research: Atmospheres, 121, 13,784-713,798, 10.1002/2016jd025252, 2016b.

Li, Z., Lee, K.-H., Wang, Y., Xin, J., and Hao, W.-M.: First observation-based estimates of cloud-free aerosol radiative forcing across China, 115, 10.1029/2009jd013306, 2010.

Li, Z., Guo, J., Ding, A., Liao, H., Liu, J., Sun, Y., Wang, T., Xue, H., Zhang, H., and Zhu, B.: Aerosol and boundary-layer interactions and impact on air quality, National Science Review, 4, 810-833, 10.1093/nsr/nwx117, 2017b.

Liu, S., Aiken, A. C., Gorkowski, K., Dubey, M. K., Cappa, C. D., Williams, L. R., Herndon, S. C., Massoli, P., Fortner, E. C., Chhabra, P. S., Brooks, W. A., Onasch, T. B., Jayne, J. T., Worsnop, D. R., China, S., Sharma, N., Mazzoleni, C., Xu, L., Ng, N. L., Liu, D., Allan, J. D., Lee, J. D., Fleming, Z. L., Mohr, C., Zotter, P., Szidat, S., and Prévôt, A. S. H.: Enhanced light absorption by mixed source black and brown carbon particles in UK winter, Nature Communications, 6, 8435, 10.1038/ncomms9435

https://www.nature.com/articles/ncomms9435#supplementary-information, 2015.

Liu, Z., Hu, B., Zhang, J., Yu, Y., and Wang, Y.: Characteristics of aerosol size distributions and chemical compositions during wintertime pollution episodes in Beijing, Atmospheric Research, 168, 1-12, 10.1016/j.atmosres.2015.08.013, 2016.

Meng, Z. Y., Ding, G. A., Xu, X. B., Xu, X. D., Yu, H. Q., and Wang, S. F.: Vertical distributions of SO(2) and NO(2) in the lower atmosphere in Beijing urban areas, China, Sci Total Environ, 390, 456-465, 10.1016/j.scitotenv.2007.10.012, 2008.

Merikallio, S., Lindqvist, H., Nousiainen, T., and Kahnert, M.: Modelling light scattering by mineral dust using spheroids: assessment of applicability, Atmospheric Chemistry and Physics, 11, 5347-5363, 10.5194/acp-11-5347-2011, 2011.

Müller, A., Miyazaki, Y., Aggarwal, S. G., Kitamori, Y., Boreddy, S. K. R., and Kawamura, K.: Effects of chemical composition and mixing state on size-resolved hygroscopicity and cloud condensation nuclei activity of submicron aerosols at a suburban site in northern Japan in summer, Journal of Geophysical Research: Atmospheres, 122, 9301-9318, 10.1002/2017jd027286, 2017.

Niu, H., Shao, L., and Zhang, D.: Soot particles at an elevated site in eastern China during the passage of a strong cyclone, Sci Total Environ, 430, 217-222, 10.1016/j.scitotenv.2012.04.050, 2012.

Niu, H., Hu, W., Zhang, D., Wu, Z., Guo, S., Pian, W., Cheng, W., and Hu, M.: Variations of fine particle physiochemical properties during a heavy haze episode in the winter of Beijing, Sci Total Environ, 571,

https://doi.org/10.5194/acp-2020-1031
Preprint. Discussion started: 30 November 2020

103-109, 10.1016/j.scitotenv.2016.07.147, 2016.

Peng, J., Hu, M., Guo, S., Du, Z., Zheng, J., Shang, D., Levy Zamora, M., Zeng, L., Shao, M., Wu, Y. S., Zheng, J., Wang, Y., Glen, C. R., Collins, D. R., Molina, M. J., and Zhang, R.: Markedly enhanced absorption and direct radiative forcing of black carbon under polluted urban environments, Proc Natl Acad Sci U S A, 113, 4266-4271, 10.1073/pnas.1602310113, 2016.

Petaja, T., Jarvi, L., Kerminen, V. M., Ding, A. J., Sun, J. N., Nie, W., Kujansuu, J., Virkkula, A., Yang, X. Q., Fu, C. B., Zilitinkevich, S., and Kulmala, M.: Enhanced air pollution via aerosol-boundary layer feedback in China, Sci Rep, 6, 18998, 10.1038/srep18998, 2016.

Platis, A., Altstädter, B., Wehner, B., Wildmann, N., Lampert, A., Hermann, M., Birmili, W., and Bange, J.: An Observational Case Study on the Influence of Atmospheric Boundary-Layer Dynamics on New Particle Formation, Boundary-Layer Meteorology, 158, 67-92, 10.1007/s10546-015-0084-y, 2015.

Qi, X., Ding, A., Nie, W., Chi, X., Huang, X., Xu, Z., Wang, T., Wang, Z., Wang, J., Sun, P., Zhang, Q., Huo, J., Wang, D., Bian, Q., Zhou, L., Zhang, Q., Ning, Z., Fei, D., Xiu, G., and Fu, Q.: Direct measurement of new particle formation based on tethered airship around the top of the planetary boundary layer in eastern China, Atmospheric Environment, 209, 92-101, 10.1016/j.atmosenv.2019.04.024, 2019.

Ramanathan, V., Crutzen, P. J., Mitra, A. P., and Sikka, D.: The Indian Ocean Experiment and the Asian Brown Cloud, Curr. Sci., 83, 947-955, 2002.

Rodriguez-Navarro, C., di Lorenzo, F., and Elert, K.: Mineralogy and physicochemical features of Saharan dust wet deposited in the Iberian Peninsula during an extreme red rain event, Atmospheric Chemistry and Physics, 18, 10089-10122, 10.5194/acp-18-10089-2018, 2018.

Saliba, G., Subramanian, R., Saleh, R., Ahern, A. T., Lipsky, E. M., Tasoglou, A., Sullivan, R. C., Bhandari, J., Mazzoleni, C., and Robinson, A. L.: Optical properties of black carbon in cookstove emissions coated with secondary organic aerosols: Measurements and modeling, Aerosol Science and Technology, 50, 1264-1276, 10.1080/02786826.2016.1225947, 2016.

Scarnato, B. V., Vahidinia, S., Richard, D. T., and Kirchstetter, T. W.: Effects of internal mixing and aggregate morphology on optical properties of black carbon using a discrete dipole approximation model, Atmospheric Chemistry and Physics, 13, 5089-5101, 10.5194/acp-13-5089-2013, 2013.

Schneider, C. A., Rasband, W. S., and Eliceiri, K. W.: NIH Image to ImageJ: 25 years of image analysis, Nature Methods, 9, 671-675, 10.1038/nmeth.2089, 2012.

Shao, L., Hou, C., Geng, C., Liu, J., Hu, Y., Wang, J., Jones, T., Zhao, C., and BéruBé, K.: The oxidative potential of PM 10 from coal, briquettes and wood charcoal burnt in an experimental domestic stove, Atmospheric Environment, 127, 372-381, 10.1016/j.atmosenv.2015.12.007, 2016.

Shao, L., Hu, Y., Shen, R., Schafer, K., Wang, J., Wang, J., Schnelle-Kreis, J., Zimmermann, R., BeruBe, K., and Suppan, P.: Seasonal variation of particle-induced oxidative potential of airborne particulate matter in Beijing, Sci Total Environ, 579, 1152-1160, 10.1016/j.scitotenv.2016.11.094, 2017.

Sharma, N., China, S., Bhandari, J., Gorkowski, K., Dubey, M., Zaveri, R. A., and Mazzoleni, C.: Physical Properties of Aerosol Internally Mixed With Soot Particles in a Biogenically Dominated Environment in California, Geophysical Research Letters, 45, 11,473-411,482, 10.1029/2018gl079404, 2018.

https://doi.org/10.5194/acp-2020-1031
Preprint. Discussion started: 30 November 2020

496 Shi, Z., Vu, T., Kotthaus, S., Harrison, R. M., Grimmond, S., Yue, S., Zhu, T., Lee, J., Han, Y., Demuzere, M.,
497 Dunmore, R. E., Ren, L., Liu, D., Wang, Y., Wild, O., Allan, J., Acton, W. J., Barlow, J., Barratt, B., Beddows,
498 D., Bloss, W. J., Calzolai, G., Carruthers, D., Carslaw, D. C., Chan, Q., Chatzidiakou, L., Chen, Y., Crilley, L.,
499 Coe, H., Dai, T., Doherty, R., Duan, F., Fu, P., Ge, B., Ge, M., Guan, D., Hamilton, J. F., He, K., Heal, M.,
500 Heard, D., Hewitt, C. N., Hollaway, M., Hu, M., Ji, D., Jiang, X., Jones, R., Kalberer, M., Kelly, F. J., Kramer,
501 L., Langford, B., Lin, C., Lewis, A. C., Li, J., Li, W., Liu, H., Liu, J., Loh, M., Lu, K., Lucarelli, F., Mann, G.,
502 McFiggans, G., Miller, M. R., Mills, G., Monk, P., Nemitz, E., amp, apos, Connor, F., Ouyang, B., Palmer, P.
503 I., Percival, C., Popoola, O., Reeves, C., Rickard, A. R., Shao, L., Shi, G., Spracklen, D., Stevenson, D., Sun,
504 Y., Sun, Z., Tao, S., Tong, S., Wang, Q., Wang, W., Wang, X., Wang, X., Wang, Z., Wei, L., Whalley, L., Wu,
505 X., Wu, Z., Xie, P., Yang, F., Zhang, Q., Zhang, Y., Zhang, Y., and Zheng, M.: Introduction to the special
506 issue “In-depth study of air pollution sources and processes within Beijing and its surrounding region
507 (APHH-Beijing)”, Atmospheric Chemistry and Physics, 19, 7519-7546, 10.5194/acp-19-7519-2019, 2019.

508 Shou, Y., Huang, Y., Zhu, X., Liu, C., Hu, Y., and Wang, H.: A review of the possible associations between
509 ambient PM2.5 exposures and the development of Alzheimer's disease, Ecotoxicol Environ Saf, 174,
510 344-352, 10.1016/j.ecoenv.2019.02.086, 2019.

511 Sorensen, C.M., 2001. Light Scattering by Fractal Aggregates: A Review. Aerosol Science and Technology,
512 35(2): 648-687.

513 Sun, Y., Zhuang, G., Tang, A., Wang, Y., and An, Z.: Chemical Characteristics of PM2.5 and PM10 in
514 Haze−Fog Episodes in Beijing, Environmental Science & Technology, 40, 3148-3155, 10.1021/es051533g,
515 2006.

516 Sun, Y., Jiang, Q., Wang, Z., Fu, P., Li, J., Yang, T., and Yin, Y.: Investigation of the sources and evolution
517 processes of severe haze pollution in Beijing in January 2013, Journal of Geophysical Research:
518 Atmospheres, 119, 4380-4398, 10.1002/2014jd021641, 2014.

519 Sun, Y., Du, W., Wang, Q., Zhang, Q., Chen, C., Chen, Y., Chen, Z., Fu, P., Wang, Z., Gao, Z., and Worsnop,
520 D. R.: Real-Time Characterization of Aerosol Particle Composition above the Urban Canopy in Beijing:
521 Insights into the Interactions between the Atmospheric Boundary Layer and Aerosol Chemistry, Environ
522 Sci Technol, 49, 11340-11347, 10.1021/acs.est.5b02373, 2015.

523 Sun, Y., Du, W., Fu, P., Wang, Q., Li, J., Ge, X., Zhang, Q., Zhu, C., Ren, L., Xu, W., Zhao, J., Han, T., Worsnop,
524 D. R., and Wang, Z.: Primary and secondary aerosols in Beijing in winter: sources, variations and

525 processes, Atmospheric Chemistry and Physics, 16, 8309-8329, 10.5194/acp-16-8309-2016, 2016.

526 Sun, Y. L., Wang, Z. F., Fu, P. Q., Yang, T., Jiang, Q., Dong, H. B., Li, J., and Jia, J. J.: Aerosol composition,
527 sources and processes during wintertime in Beijing, China, Atmospheric Chemistry and Physics, 13,
528 4577-4592, 10.5194/acp-13-4577-2013, 2013.

529 Tang, M., Cziczo, D. J., and Grassian, V. H.: Interactions of Water with Mineral Dust Aerosol: Water
530 Adsorption, Hygroscopicity, Cloud Condensation, and Ice Nucleation, Chem Rev, 116, 4205-4259,
531 10.1021/acs.chemrev.5b00529, 2016.

532 Tao, J., Zhang, L., Cao, J., and Zhang, R.: A review of current knowledge concerning
533 PM_{2. 5} chemical composition, aerosol optical properties and their relationships
534 across China, Atmospheric Chemistry and Physics, 17, 9485-9518, 10.5194/acp-17-9485-2017, 2017.

https://doi.org/10.5194/acp-2020-1031
Preprint. Discussion started: 30 November 2020

Atmospheric Chemistry and Physics Discussions

Unga, F., Choël, M., Derimian, Y., Deboudt, K., Dubovik, O., and Goloub, P.: Microscopic Observations of Core - Shell Particle Structure and Implications for Atmospheric Aerosol Remote Sensing, Journal of Geophysical Research: Atmospheres, 123, 13,944-913,962, 10.1029/2018jd028602, 2018.

Wang, G., Zhang, R., Gomez, M. E., Yang, L., Levy Zamora, M., Hu, M., Lin, Y., Peng, J., Guo, S., Meng, J., Li, J., Cheng, C., Hu, T., Ren, Y., Wang, Y., Gao, J., Cao, J., An, Z., Zhou, W., Li, G., Wang, J., Tian, P., Marrero-Ortiz, W., Secrest, J., Du, Z., Zheng, J., Shang, D., Zeng, L., Shao, M., Wang, W., Huang, Y., Wang, Y., Zhu, Y., Li, Y., Hu, J., Pan, B., Cai, L., Cheng, Y., Ji, Y., Zhang, F., Rosenfeld, D., Liss, P. S., Duce, R. A., Kolb, C. E., and Molina, M. J.: Persistent sulfate formation from London Fog to Chinese haze, Proc Natl Acad Sci U S A, 113, 13630-13635, 10.1073/pnas.1616540113, 2016.

Wang, Q., Sun, Y., Xu, W., Du, W., Zhou, L., Tang, G., Chen, C., Cheng, X., Zhao, X., Ji, D., Han, T., Wang, Z., Li, J., and Wang, Z.: Vertically resolved characteristics of air pollution during two severe winter haze episodes in urban Beijing, China, Atmospheric Chemistry and Physics, 18, 2495-2509, 10.5194/acp-18-2495-2018, 2018.

Wang, W., Shao, L., Guo, M., Hou, C., Xing, J., and Wu, F.: Physicochemical Properties of Individual Airborne Particles in Beijing during Pollution Periods, Aerosol and Air Quality Research, 17, 3209-3219, 10.4209/aaqr.2017.03.0116, 2017.

Wang, X., Cotter, E., Iyer, K. N., Fang, J., Williams, B. J., and Biswas, P.: Relationship between pyrolysis products and organic aerosols formed during coal combustion, Proceedings of the Combustion Institute, 35, 2347-2354, 10.1016/j.proci.2014.07.073, 2015.

Wang, Y., Yao, L., Wang, L., Liu, Z., Ji, D., Tang, G., Zhang, J., Sun, Y., Hu, B., and Xin, J.: Mechanism for the formation of the January 2013 heavy haze pollution episode over central and eastern China, Science China Earth Sciences, 57, 14-25, 10.1007/s11430-013-4773-4, 2013.

Wehner, B., Siebert, H., Ansmann, A., Ditas, F., Seifert, P., Stratmann, F., Wiedensohler, A., Apituley, A., Shaw, R. A., Manninen, H. E., and Kulmala, M.: Observations of turbulence-induced new particle formation in the residual layer, Atmospheric Chemistry and Physics, 10, 4319-4330, 10.5194/acp-10-4319-2010, 2010.

Li, W., Xu, L., Liu, X., Zhang, J., Lin, Y., Yao, X., Gao, H., Zhang, D., Chen, J., Wang, W., Harrison, R. M., Zhang, X., Shao, L., Fu, P.: Athanasios Nenes, and Zongbo Shi: Air pollution–aerosol interactions produce more bioavailable iron for ocean ecosystems, Science Advance, 3, e1601749, 2017.

Xia, Y., Guan, D., Meng, J., Li, Y., and Shan, Y.: Assessment of the pollution–health–economics nexus in China, Atmospheric Chemistry and Physics, 18, 14433-14443, 10.5194/acp-18-14433-2018, 2018.

Xu, L., Liu, L., Zhang, J., Zhang, Y., Ren, Y., Wang, X., and Li, W.: Morphology, Composition, and Mixing State of Individual Aerosol Particles in Northeast China during Wintertime, Atmosphere, 8, 10.3390/atmos8030047, 2017.

Xu, L., Zhang, D., and Li, W.: Microscopic comparison of aerosol particles collected at an urban site in North China and a coastal site in Japan, Sci Total Environ, 669, 948-954, 10.1016/j.scitotenv.2019.03.163, 2019.

Yuan, Q., Li, W., Zhou, S., Yang, L., Chi, J., Sui, X., and Wang, W.: Integrated evaluation of aerosols during haze-fog episodes at one regional background site in North China Plain, Atmospheric Research, 156,

https://doi.org/10.5194/acp-2020-1031
Preprint. Discussion started: 30 November 2020

574 102-110, 10.1016/j.atmosres.2015.01.002, 2015.

575 Zhang, J., Liu, L., Wang, Y., Ren, Y., Wang, X., Shi, Z., Zhang, D., Che, H., Zhao, H., Liu, Y., Niu, H., Chen, J.,
576 Zhang, X., Lingaswamy, A. P., Wang, Z., and Li, W.: Chemical composition, source, and process of urban
577 aerosols during winter haze formation in Northeast China, Environ Pollut, 231, 357-366,
578 10.1016/j.envpol.2017.07.102, 2017.

579 Zhang, J., Liu, L., Xu, L., Lin, Q., Zhao, H., Wang, Z., Guo, S., Hu, M., Liu, D., Shi, Z., Huang, D., and Li, W.:
580 Exploring wintertime regional haze in northeast China: role of coal and biomass burning, Atmos. Chem.
581 Phys., 20, 5355-5372, 10.5194/acp-20-5355-2020, 2020.

582 Zhang, Q., Ma, X., Tie, X., Huang, M., and Zhao, C.: Vertical distributions of aerosols under different
583 weather conditions: Analysis of in-situ aircraft measurements in Beijing, China, Atmospheric
584 Environment, 43, 5526-5535, https://doi.org/10.1016/j.atmosenv.2009.05.037, 2009.

585 Zhou, W., Sun, Y., Xu, W., Zhao, X., Wang, Q., Tang, G., Zhou, L., Chen, C., Du, W., Zhao, J., Xie, C., Fu, P.,
586 and Wang, Z.: Vertical Characterization of Aerosol Particle Composition in Beijing, China: Insights From
587 3 - Month Measurements With Two Aerosol Mass Spectrometers, Journal of Geophysical Research:
588 Atmospheres, 123, 13,016-013,029, 10.1029/2018jd029337, 2018a.

589 Zhou, W., Wang, Q., Zhao, X., Xu, W., Chen, C., Du, W., Zhao, J., Canonaco, F., Prévôt, A. S. H., Fu, P.,
590 Wang, Z., Worsnop, D. R., and Sun, Y.: Characterization and source apportionment of organic aerosol at
591 260 m on a meteorological tower in Beijing, China, Atmospheric Chemistry and Physics, 18,
592 3951-3968, 10.5194/acp-18-3951-2018, 2018b.

593 Zhu, J., Crozier, P. A., and Anderson, J. R.: Characterization of light-absorbing carbon particles at three
594 altitudes in East Asian outflow by transmission electron microscopy, Atmospheric Chemistry and Physics,
595 13, 6359-6371, 10.5194/acp-13-6359-2013, 2013.

596

https://doi.org/10.5194/acp-2020-1031
Preprint. Discussion started: 30 November 2020

Atmospheric Chemistry and Physics Discussions

597 Table 1 Sample information and meteorological conditions

Sample ID①	Date (2016)	Time ②	$PM_{2.5}$ (μg m^{-3})	SO_2 (μg m^{-3})	NO_2 (μg m^{-3})	O_3 (μg m^{-3})	RH (%)	T (℃)	MLH (m)③
Z1-1	12/1	9:10	12④	2	48	37	24	6	--
Z2-1	12/1	8:40	--	--	--	--	--	--	194
Z1-2	12/2	1:00	110	25	109	3	55	2	--
Z2-2	12/2	1:00	--	--	--	--	--	--	141
Z1-3	12/2	9:10	24	20	134	2	50	3	--
Z2-3	12/2	8:40	--	--	--	--	--	--	134
Z1-4	12/3	1:53	142	36	102	6	79	-1	--
Z2-4	12/3	3:00	--	--	--	--	--	--	232
Z1-5	12/4	1:04	530	14	180	4	93	1	--
Z2-5	12/4	3:00	--	--	--	--	--	--	136
Z1-6	12/5	2:00	86	8	21	53	75	2	--
Z2-6	12/5	2:00	--	--	--	--	--	--	114
Z1-7	12/8	9:10	187	2	16	72	86	2	--
Z2-7	12/8	8:40	--	--	--	--	--	--	191
Z1-8	12/9	9:20	12	8	67	12	33	2	--
Z2-8	12/9	8:30	--	--	--	--	--	--	250

598 ①Samples were collected at two altitudes: Z1 was 2 m above ground and Z2 was 280 m above
599 ground. ② Sampling duration ranged from 30 s to less than 5 minutes depending on the PM
600 pollution. ③ MLH represents the mixed layer height and the data are 15minutes average; MLH
601 was less than 280 m and the samples collected at Z2 represent samples above the mixed layer. ④
602 If $PM_{2.5}$ mass concentration was less than 75 μg m^{-3}, samples were classified as non-haze samples
603 and if $PM_{2.5}$ mass concentration was more than 75 μg m^{-3}, samples were classified as haze samples.
604

https://doi.org/10.5194/acp-2020-1031
Preprint. Discussion started: 30 November 2020

Atmospheric Chemistry and Physics Discussions

605 Table 2 Classification and characteristics of individual particle types.

Particle type	Elemental composition	Morphology	Possible sources
Soot particles	C and minor amounts of O, Si.	Chain-like or compact C-dominated aggregates.	Incomplete combustion of biomass and fossil fuel.
Organic particles	C and O with minor amounts of Si, K, S, Cl.	Spherical, near spherical or irregular shapes.	Combustion process or secondary aerosol formation.
Mineral particles	O, Si, Al, Ca, Fe, Na, K, Mg, Ti, and S.	Irregular shapes.	Re-suspended from soil dust, road dust, and construction dust.
Metal particles	Fe, Zn, Mn, Ti, and Pb.	Spherical or irregular shapes.	Industries, coal-fired power plants and oil refineries.
S-rich particles	S and O with minor amounts of N, K.	Spherical, near spherical or irregular shapes.	Secondary aerosol formation.
Organic mixed with Sulfur-rich particles	C, O, and S with minor amounts of N, K or Cl.	Irregular shapes.	Secondary aerosol reaction.
Other mixed particles	Complex elemental composition.	Irregular shapes with different particle types.	Secondary aerosol reaction.

606

https://doi.org/10.5194/acp-2020-1031
Preprint. Discussion started: 30 November 2020

Atmospheric Chemistry and Physics Discussions

607 Table 3 Relative number percentage of individual particles.

Air qualities	Sample ID	Number	Metals	Minerals	OPs	S-rich	Soot	OP-S	Other
Non-haze periods	Z1-1	114	2.6	30.7	19.3	36.0	5.3	1.8	4.4
	Z2-1	113	1.8	12.4	16.8	56.6	10.6	0.9	0.9
	Z1-3	135	4.4	34.1	31.9	12.6	11.1	0.7	5.2
	Z2-3	118	2.5	23.7	45.8	17.0	4.2	2.5	4.2
	Z1-8	140	1.4	62.9	12.1	11.4	2.9	2.1	7.1
	Z2-8	119	3.4	33.6	19.3	18.5	17.7	0.0	7.6
	Ave (Z1)	389	2.8	42.5	21.1	20.0	6.4	1.6	5.6
	Ave (Z2)	350	2.6	23.2	27.3	30.7	10.8	1.1	4.2
Haze periods	Z1-2	123	2.4	21.1	42.3	17.1	7.3	2.4	7.3
	Z2-2	164	4.9	14.6	37.2	25.0	4.3	9.8	4.3
	Z1-4	160	0.6	28.8	30.6	8.8	13.8	9.4	8.1
	Z2-4	266	0.0	3.8	53.0	3.4	7.1	19.6	13.2
	Z1-5	461	0.9	6.5	18.9	22.1	7.6	31.5	12.6
	Z2-5	266	0.4	0.4	32.3	7.1	2.3	44.0	13.5
	Z1-6	237	2.5	11.0	21.5	48.5	2.1	6.8	7.6
	Z2-6	281	1.8	11.0	18.9	19.6	12.8	15.3	20.6
	Z1-7	168	1.8	23.2	28.0	20.8	2.4	15.5	8.3
	Z2-7	192	1.6	17.7	32.3	27.1	1.6	15.1	4.7
	Ave (Z1)	1149	1.7	18.1	28.3	23.5	6.6	13.1	8.8
	Ave (Z2)	1169	1.7	9.5	34.7	16.4	5.6	20.7	11.3

608

https://doi.org/10.5194/acp-2020-1031
Preprint. Discussion started: 30 November 2020

Atmospheric Chemistry and Physics Discussions

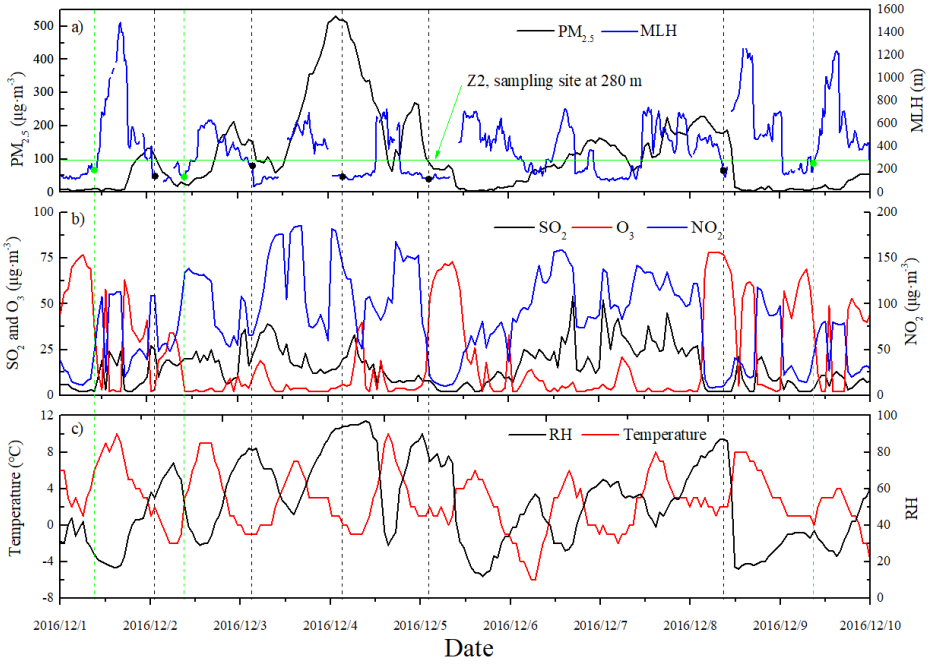

Fig. 1: The dashed lines represent the individual particle sampling times with green lines representing non-haze samples and black lines haze samples. (a) Temporal variations of mixed layer height (MLH) and $PM_{2.5}$ mass concentrations. The solid dots represent the MLH during the sampling times. (b) Temporal variations of SO_2, NO_2, O_3 at ground level at the Olympic Park monitor site, which is the closest national air quality monitor station to the sampling site (~1.5 km). (c) Temporal variations of temperature (T) and relative humidity (RH) at ground level. Date were obtained from the Ministry of Ecology and Environment of China (https://www.aqistudy.cn);

https://doi.org/10.5194/acp-2020-1031
Preprint. Discussion started: 30 November 2020

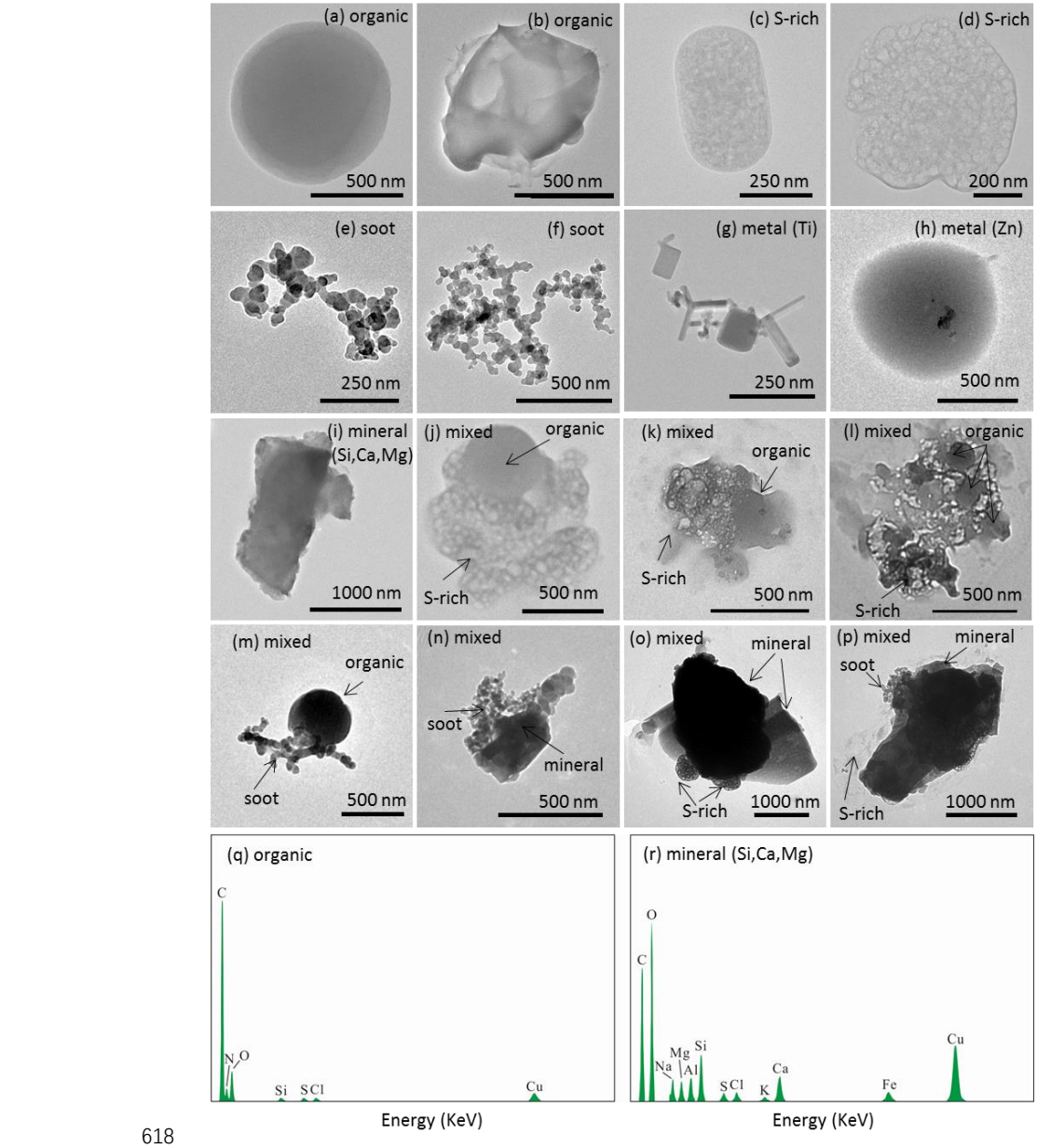

Fig. 2: Examples of morphologies and mixing characteristics of individual aerosol particles in winter in Beijing at ground level and above the mixed layer. (a) Spherical organic particle, (b) irregular shaped organic particle, (c-d) S-rich particles, (e-f) soot particles, (g-h) metal particles, (i) mineral particles, (j-l) OP-S mixed particles, and (m-p) other mixed particle types. (q) and (r) are EDS of (b) and (i). The difference between the particles in (b) and (i) is that organic particles (b) mainly composed C and O while minerals (i) mainly composed O, Si, Ca and Mg.

https://doi.org/10.5194/acp-2020-1031
Preprint. Discussion started: 30 November 2020

Atmospheric Chemistry and Physics Discussions

626

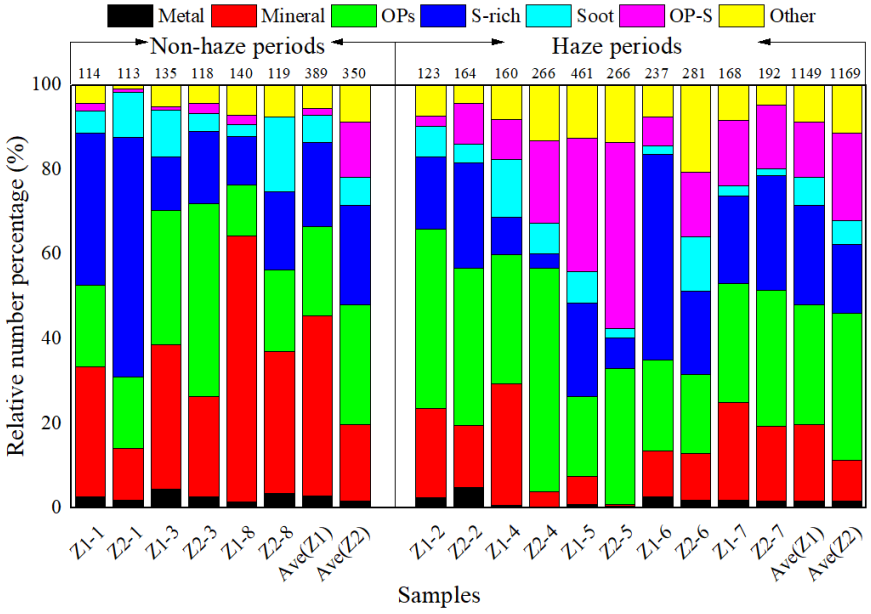

627

628 Fig. 3: Relative number percentage of different particle types at ground level (Z1) and above the
629 mixed layer height (Z2). The number above each bar represents the total particle number analyzed
630 in each sample.

https://doi.org/10.5194/acp-2020-1031
Preprint. Discussion started: 30 November 2020

Atmospheric Chemistry and Physics Discussions

631

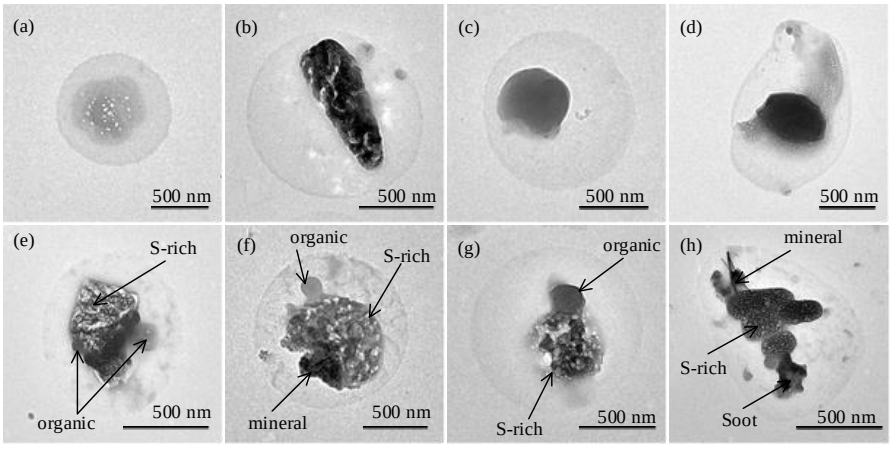

632

633 Fig. 4: Images of core-shell structured particles. (a-b) S-rich cores, (c-d) organic cores, and (e-h)
634 mixed cores.

https://doi.org/10.5194/acp-2020-1031
Preprint. Discussion started: 30 November 2020

Atmospheric Chemistry and Physics Discussions

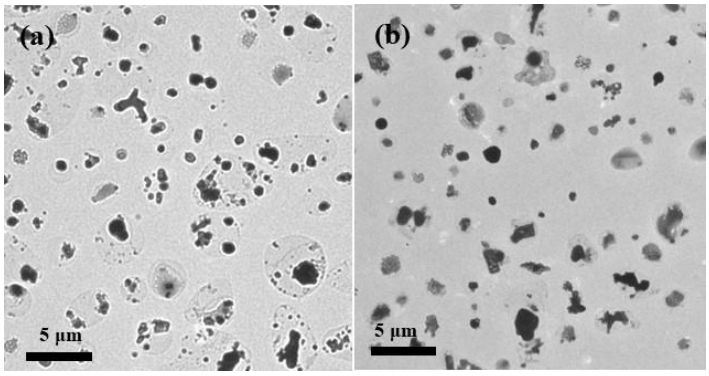

635
636 Fig. 5 Low magnification images of individual particles during haze periods above the MLH (a)
637 and at ground level (b). More coated particles are shown above the MLH.

https://doi.org/10.5194/acp-2020-1031
Preprint. Discussion started: 30 November 2020

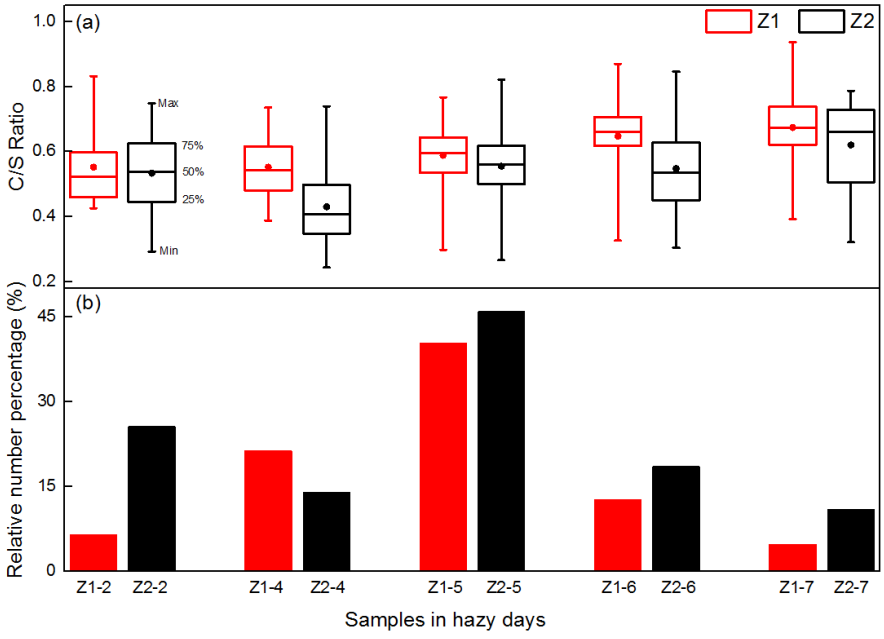

Fig. 6: (a) C/S ratio (D_{Aeq} ratio of the core to the whole particle including the shell) of particles during haze periods at ground level (Z1) and above the mixed layer height (Z2); solid dots represent the average value, and (b) the corresponding relative number percentage of core-shell structured particles.

https://doi.org/10.5194/acp-2020-1031
Preprint. Discussion started: 30 November 2020

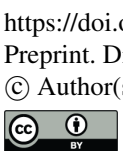

Atmospheric Chemistry and Physics Discussions

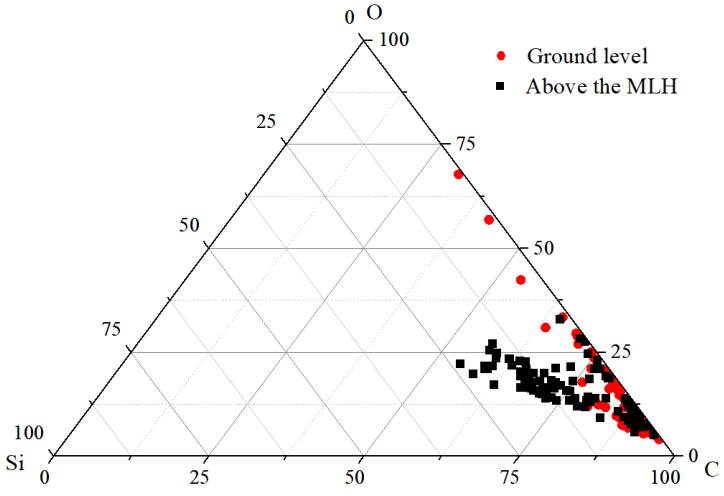

643
644
645 Fig. 7: Triangular diagram showing the weight ratio of C-O-Si of organic particles at ground level
646 and above the mixed layer height (MLH).